Human Molecular Genetics, 1997, Vol. 6, No. 4 527–537

Co-ordinate regulation of the cystic fibrosis and multidrug resistance genes in cystic fibrosis knockout mice

Ann E. O. Trezise[1,*], Rosemary Ratcliff[2], Tim E. Hawkins[2], Martin J. Evans[2], Tom C. Freeman[3], Pascale R. Romano[1], Christopher F. Higgins[1] and William H. Colledge[4]

[1]Nuffield Department of Clinical Biochemistry and Imperial Cancer Research Fund Laboratories, Institute of Molecular Medicine, University of Oxford, John Radcliffe Hospital, Oxford OX3 9DU, UK, [2]Wellcome/CRC Institute of Cancer and Developmental Biology, University of Cambridge, Tennis Court Road, Cambridge CB2 1QR, UK, [3]Human Genetics Group, The Sanger Centre, Wellcome Trust Genome Campus, Hinxton, Cambs CB10 1SA, UK and [4]Physiological Laboratory, University of Cambridge, Downing St, Cambridge CB2 3EG, UK

Received October 17, 1996; Revised and Accepted January 10, 1997

The cystic fibrosis (*Cftr*) and multidrug resistance (*Mdr1*) genes encode structurally similar proteins which are members of the ABC transporter superfamily. These genes exhibit complementary patterns of expression *in vivo*, suggesting that the regulation of their expression may be co-ordinated. We have tested this hypothesis *in vivo* by examining *Cftr* and *Mdr1* expression in cystic fibrosis knockout transgenic mice (*Cftr*^{tm1CAM}). Cftr mRNA expression in *Cftr*^{tm1CAM}/*Cftr*^{tm1CAM} mice was 4-fold reduced in the intestine, as compared with littermate wild-type mice. All other *Cftr*^{tm1CAM}/*Cftr*^{tm1CAM} mouse tissues examined showed similar reductions in *Cftr* expression. In contrast, we observed a 4-fold increase in Mdr1 mRNA expression in the intestines of neonatal and 3- to 4-week-old *Cftr*^{tm1CAM}/*Cftr*^{tm1CAM} mice, as compared with age-matched +/+ mice, and an intermediate level of Mdr1 mRNA in heterozygous *Cftr*^{tm1CAM} mice. In 10-week-old, *Cftr*^{tm1CAM}/*Cftr*^{tm1CAM} mice and in contrast to the younger mice, Mdr1 mRNA expression was reduced, by 3-fold. The expression of two control genes, *Pgk-1* and *Mdr2*, was similar in all genotypes, suggesting that the changes in Mdr1 mRNA levels observed in the *Cftr*^{tm1CAM}/*Cftr*^{tm1CAM} mice are specific to the loss of *Cftr* expression and/or function. These data provide further evidence supporting the hypothesis that the regulation *Cftr* and *Mdr1* expression is co-ordinated *in vivo,* and that this co-ordinate regulation is influenced by temporal factors.

INTRODUCTION

Mutations in the cystic fibrosis transmembrane conductance regulator gene (*CFTR*) cause cystic fibrosis (1–3). Cystic fibrosis affects a number of organ systems, including the respiratory, digestive and reproductive systems (4), and its underlying cause is the aberrant expression and/or function of a cAMP-regulated chloride channel encoded by *CFTR* (5–7). As well as functioning as a chloride channel, CFTR also regulates other ion channels (8,9).

The primary structure of CFTR places it in the ABC transporter superfamily (2,10). The P-glycoproteins, encoded by the *MDR1* and *MDR2* genes in humans and by the *Mdr1a*, *Mdr1b* and *Mdr2* genes in rodents, are also members of the ABC transporter superfamily (reviewed in 11). The P-glycoproteins encoded by human *MDR1* and mouse *Mdr1a* and *Mdr1b* can confer multidrug resistance by transporting chemotherapeutic drugs out of cells. In addition to their drug transport function, human MDR1 and mouse Mdr1a modulate the activation of cell swelling-activated chloride channels (12–14). Thus, the *Cftr* and *Mdr1* genes are structurally related, sharing a common domain organisation, and functionally related, acting as regulators of heterologous ion channels.

We have shown previously that *Cftr* and *Mdr1a* and/or *1b* (collectively referred to as *Mdr1*) exhibit complementary patterns of expression *in vivo* (5). That is, in cells which express *Cftr*, *Mdr1* expression cannot be detected, and vice versa. Furthermore, during development and differentiation, certain cells switch expression from one gene to the other. For example, *Cftr* is expressed in the epithelia of the intestinal crypts while *Mdr1* is expressed in the villous epithelia. As the epithelial cells migrate across the crypt–villous boundary, *Cftr* expression is reduced to undetectable levels while *Mdr1* expression is switched on. Similarly, *Cftr* is expressed in the uterine epithelia during the oestrous cycle; then at the onset of pregnancy these cells turn off expression of *Cftr* and switch on *Mdr1* expression. These findings led us to propose that the regulation of *Cftr* and *Mdr1* expression may be co-ordinated (15). A number of *in vitro* studies also suggest co-ordinate regulation of *Cftr* and *Mdr1* expression. Galactose-induced differentiation of HT-29 cells (human intestinal cell line) is accompanied by opposite shifts in *CFTR* and *MDR1* expression (16). Similarly, colchicine induction of *MDR1*

*To whom correspondence should be addressed

expression is accompanied by an 80% decrease in *CFTR* expression. Both effects are reversed following removal of the drug (17).

The creation of cystic fibrosis knockout transgenic mice has allowed us to test the co-ordinate regulation hypothesis *in vivo*. Cystic fibrosis knockout transgenic mice have been constructed, independently, by several groups (18–23). We have used RNA *in situ* hybridisation to examine *Cftr* and *Mdr1* expression in the *Cftr*^{tm1CAM} null mice (19). These mice were created using a replacement targeting strategy and have a severe cystic fibrosis phenotype with most animals succumbing to intestinal blockages early in life. No Cftr-related chloride conductances can be detected in the intestinal, tracheal or pancreatic duct epithelia of *Cftr*^{tm1CAM}/*Cftr*^{tm1CAM} mice (18,19,24). It is possible that in the absence of *Cftr* expression/function, the cellular response may be to activate other chloride channels by increasing the expression of genes encoding chloride channel regulators, such as Mdr1. The hypothesis of co-ordinate regulation of *Cftr* and *Mdr1* expression predicts that an alteration in *Cftr* expression should lead to changes in *Mdr1* expression. Here we show that the level of Cftr mRNA is greatly reduced in all tissues examined in *Cftr*^{tm1CAM}/*Cftr*^{tm1CAM} mice, as compared with wild-type mice. This decrease in Cftr mRNA levels is accompanied by altered Mdr1 mRNA expression, providing supporting evidence for the hypothesis that expression of *Cftr* and *Mdr1* is co-ordinately regulated *in vivo*.

RESULTS

Nature of Cftr mRNAs expressed in *Cftr*^{tm1CAM} mice

We investigated the nature of the mRNAs transcribed from the *Cftr*^{tm1CAM} locus to assess the effectiveness of the transcription termination signals inserted in exon 10. Figure 1 shows the structure of part of the *Cftr*^{tm1CAM} locus surrounding the targeted disruption in exon 10, and a number of possible RNAs that could be transcribed from this gene. The Cftr promoter has not been altered in the *Cftr*^{tm1CAM} mice and, therefore, transcription initiation is not expected to be affected by the gene disruption. If RNAs initiated at the Cftr promoter are terminated at the targeted disruption, as predicted, then the transcript shown in Figure 1a would be produced. The constitutive Pgk-1 promoter, which was introduced at the targeted disruption in *Cftr* exon 10, is also expected to initiate transcription. If these transcripts are terminated at the Pgk-1 poly(A)$^+$/transcription termination signals then they would only contain a *HPRT*^{R} coding sequence (transcripts not shown). However, if the Pgk-1 poly(A)$^+$/transcription termination signals are not 100% efficient, then two other RNAs containing the *Cftr* coding sequence are predicted. One of these is initiated from the Pgk-1 promoter (Fig. 1b), and the other from the endogenous Cftr promoter (Fig. 1c). It is also possible that a Cftr mRNA spliced directly from exon 9 to exon 11 may be produced (Fig. 1d), although this would result in a frame-shift mutation and the introduction of downstream, in-frame translation stop codons. Cryptic splice sites in and around exon 10 and the targeted mutation might exist, although there is no evidence for such sites being used in the *Cftr*^{tm1CAM} mice. None of the predicted Cftr mRNAs shown in Figure 1 can encode a functional Cftr protein, and electrophysiological analysis of the *Cftr*^{tm1CAM} mice demonstrates a null Cftr phenotype (18,19,24).

We used reverse transcription-polymerase chain reaction (RT-PCR) and RNase protection analyses to investigate the nature of Cftr transcripts expressed from the *Cftr*^{tm1CAM} locus. In tissues that usually express *Cftr*, all the possible Cftr mRNAs shown in Figure 1 would be anticipated, whereas in tissues that do not usually express *Cftr* only the Cftr mRNA shown in Figure 1b is predicted. In the RT-PCR, two Cftr fragments were amplified, one from exons 4–6 upstream of the targeted disruption (Fig. 2, lanes 'u'), and the other from exons 11–13 downstream of the disruption (Fig. 2, lanes 'd'). Amplification of β-actin mRNA (Fig. 2, lanes 'a') was used as a positive control. In *Cftr*^{tm1CAM}/*Cftr*^{tm1CAM} mice, the upstream primers generated a 480 bp product from total RNA extracted from lung, kidney, uterus, testis, small intestine, colon, brain and stomach (Fig. 2, lanes 'u' and data not shown). However, no upstream product could be amplified from spleen, liver, heart and skeletal muscle RNA (Fig. 2, lanes 'u' and data not shown). So, amplification of the upstream PCR product coincides accurately with the known tissue distribution of Cftr mRNA (25,26). In +/+ mice, the downstream PCR product (375 bp) could only be amplified from RNA prepared from tissues known to express *Cftr* (Fig. 2, lanes 'd' and data not shown), whereas in the *Cftr*^{tm1CAM}/*Cftr*^{tm1CAM} mice, the downstream Cftr primers amplified a 375 bp PCR product from RNA isolated from all tissues examined, including those where no upstream PCR product was observed (Fig. 2, lanes 'd' and data not shown). Presumably, this is due to transcription initiation from the ubiquitously expressed Pgk-1 promoter (contained within the targeting construct) and some read-through of the transcription termination signals of the *HPRT*^{R} mini-gene (see Fig. 1b).

To assess the extent of transcriptional read-through of the *HPRT*^{R} mini-gene, we used RNase protection analysis with a probe specific for *Cftr* exon 10 and spanning the targeted disruption. A 191 bp RNA fragment from this probe (plasmid pE16) will be protected by wild-type Cftr mRNA and this was observed with RNA isolated from testis, kidney and intestine of +/+ and +/*Cftr*^{tm1CAM} animals, but not *Cftr*^{tm1CAM}/*Cftr*^{tm1CAM} mice (Fig.3A). A 71 bp fragment was protected by RNA isolated from the testis of *Cftr*^{tm1CAM}/*Cftr*^{tm1CAM} mice (Fig. 3A, lane –/– T and data not shown), the size predicted for RNA containing the 5′ region of *Cftr* exon 10 up to the inserted *HPRT*^{R} mini-gene. The decreased signal from this 71 bp fragment, compared with the 191 bp fragment in the +/+ mice, is due in part to the decreased size of the protected fragment, but also suggests that the amount of truncated Cftr mRNA (Fig. 1a) was greatly reduced. Inability to detect this 71 bp fragment in the kidney and intestine, which express similar Cftr mRNA levels to the testes, suggests differential stability of the truncated Cftr mRNA (Fig. 1a) in different tissues. A second probe, containing the 3′ region of exon 10 (generated from plasmid p987), would be predicted to generate a 122 bp protected fragment when hybridised either to wild-type Cftr mRNA or to the fused HPRT^R–Cftr transcripts resulting from read-through of the poly(A)$^+$ signal sequence (Fig. 1b and c). A 122 bp fragment was protected by RNA from the testis, kidney and intestine of +/+ and +/*Cftr*^{tm1CAM} animals, but not *Cftr*^{tm1CAM}/*Cftr*^{tm1CAM} animals (Fig. 3B), indicating that the only downstream sequences detected by RNase protection were from wild-type Cftr mRNA. In *Cftr*^{tm1CAM}/*Cftr*^{tm1CAM} mice, the detection of Cftr mRNAs containing sequences downstream of the targeted interruption by RT-PCR, but not by RNase protection, suggests that transcriptional read-through of the Pgk-1 termination signal is very low. This analysis establishes that the

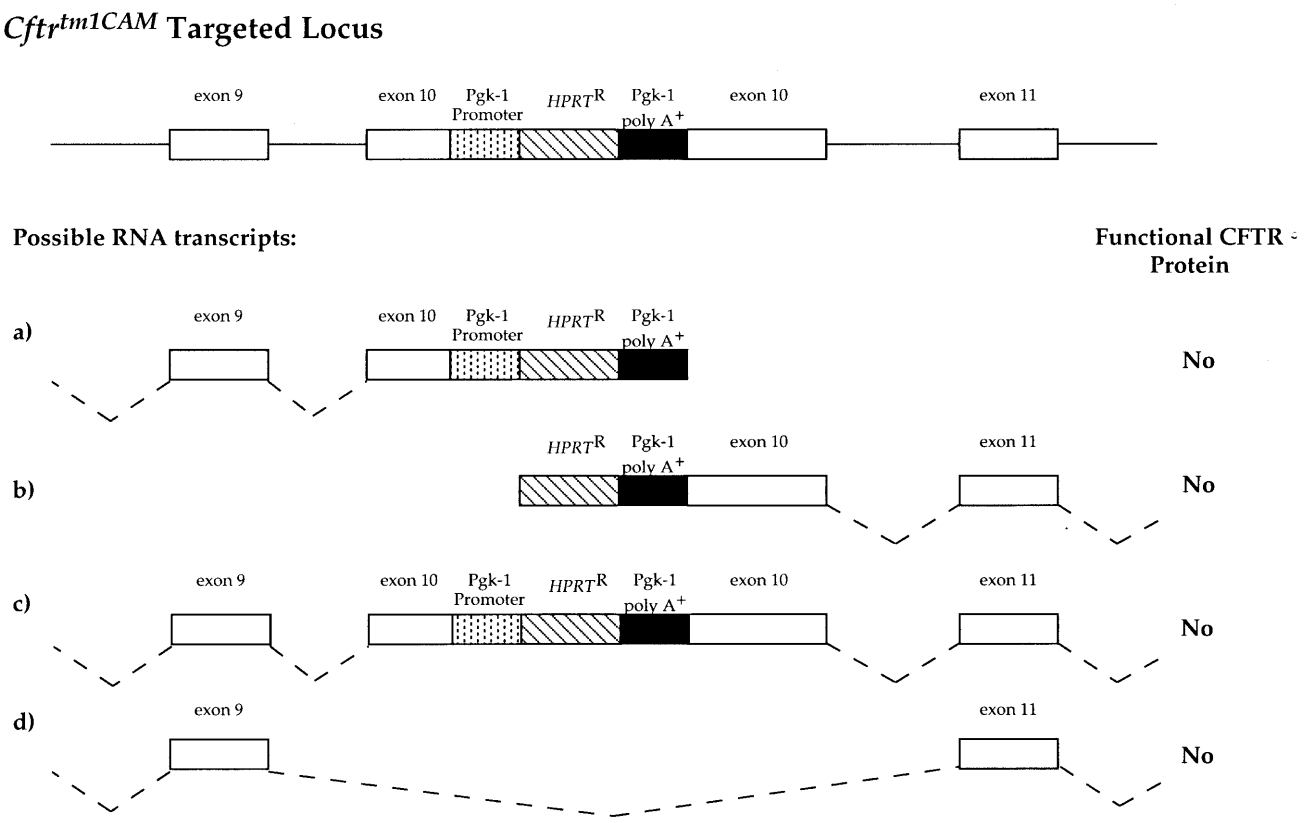

Figure 1. Diagram of exons 9–11 of the disrupted *Cftr* locus and mRNAs predicted to be expressed in *Cftr*^{tm1CAM} mice. The RNA shown in (**a**) would be predicted if RNA transcription initiated normally at the *Cftr* promoter and was terminated at the introduced mini-gene transcription termination signal. The RNAs shown in (**b**) and (**c**) would be predicted if there is read-through of the introduced mini-gene transcription termination signal. The RNA shown in (b) is initiated at the introduced Pgk-1 promoter and the RNA shown in (c) is initiated at the Cftr promoter.

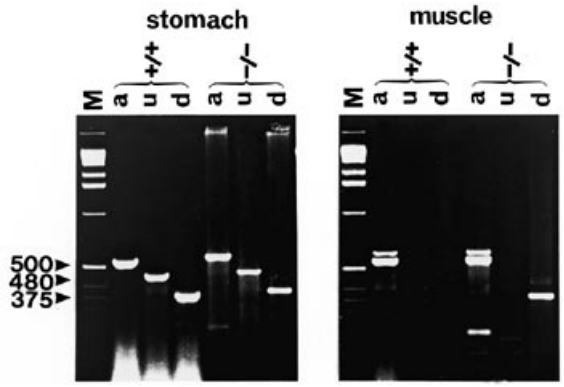

Figure 2. Reverse transcription-PCR analysis of *Cftr* expression in stomach and skeletal muscle of *Cftr*^{tm1CAM} mice. Lane a shows the products of a control amplification of β-actin mRNA sequences. Lane u shows the products of an amplification of exons 4–6 of Cftr mRNA sequences, upstream of the targeted disruption in exon 10. Lane d shows the products of an amplification of exons 11–13 of Cftr mRNA sequences downstream of the targeted disruption in exon 10. Lane M shows size standards. The sizes (bp) of the amplified fragments are shown on the left.

targeted disruption in *Cftr*^{tm1CAM} exon 10 effectively terminates the majority of transcription at this point.

Cftr expression in *Cftr*^{tm1CAM} mice

RNA *in situ* hybridisation was used to study the localisation and level of Cftr mRNA expression in *Cftr*^{tm1CAM} mice at three different stages of development: neonatal (1 day), suckling–weaning transition (3–4 weeks) and adult (10 weeks). We used two probes to examine *Cftr* expression, one upstream of the targeted disruption of the *Cftr* locus and the other downstream. The upstream Cftr probe hybridised to exons 3–5 (bp 309–695), and the downstream probe recognised exons 11–13 (bp 1771–2112 according to ref. 27). The RT-PCR and RNase protection analyses have shown that the majority of the Cftr mRNA expressed in the *Cftr*^{tm1CAM}/*Cftr*^{tm1CAM} mice was initiated at the Cftr promoter and terminated at the targeted disruption in *Cftr* exon 10 (see Fig. 1a). So, the hybridisation signal detected with the upstream Cftr probe (see Fig. 4) indicates the localisation and level of mRNAs initiated at the Cftr promoter (Fig. 1a, c and d).

In 1-day-old, +/+ mice, the upstream Cftr probe readily detected Cftr mRNA in the intestinal intervillous epithelia from which the intestinal crypts develop during postnatal weeks 1 and 2 (see Fig. 4A and B). In contrast, very little Cftr mRNA could be detected in the intestines of *Cftr*^{tm1CAM}/*Cftr*^{tm1CAM} mice (Fig. 4G and H); in +/*Cftr*^{tm1CAM} mice an intermediate amount of Cftr mRNA was observed (Fig. 4D and E). At all times, the experimenters performing the RNA *in situ* hybridisations were blinded with respect to the genotypes of the animals examined. Using RNA *in situ* hybridisation to examine Cftr mRNA levels,

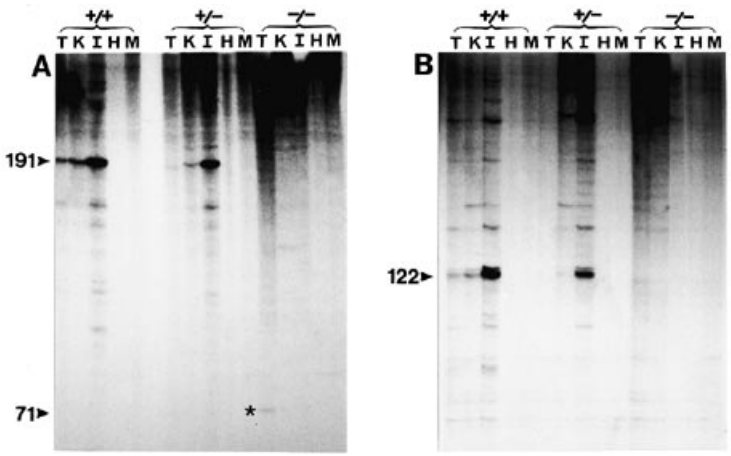

Figure 3. RNase protection analysis of *Cftr* expression in *Cftr*^{tm1CAM} mice. *Cftr* expression was analysed in testis (T), kidney (K), intestine (I), heart (H) and skeletal muscle (M). (**A**) RNase protection using a probe specific for Cftr exon 10 and spanning the targeted interruption. Arrows indicate specifically protected fragments at 191 and 71 bp. (**B**) RNase protection using a probe to the 3′ region of Cftr exon 10. The arrow indicates a specifically protected fragment at 122 bp.

the genotypes of *Cftr*^{tm1CAM} mice were identified correctly in 28/30 cases and all the *Cftr*^{tm1CAM}/*Cftr*^{tm1CAM} mice (nine) were identified correctly.

Relative levels of mRNA expression were determined objectively by densitometric analysis of X-ray film contact sheets made from slides prior to autoradiography (see Materials and Methods). This analysis showed that the hybridisation signal in 1-day-old, +/+ mice was clearly detectable, while the signal in *Cftr*^{tm1CAM}/*Cftr*^{tm1CAM} mice was not above background level.

We also examined *Cftr* expression in the intestines of 3- to 4-week-old (suckling–weaning transition) and 10-week-old (adult) mice. The results of these experiments are summarised in Table 1. Compared with +/+ mice, the upstream Cftr probe detected reduced, but still clearly detectable levels of Cftr mRNA in the submucosal (Brunner's) glands of the intestine of 3- to 4-week-old *Cftr*^{tm1CAM}/*Cftr*^{tm1CAM} mice. However, the downstream probe detected very little Cftr mRNA in the Brunner's glands of *Cftr*^{tm1CAM}/ *Cftr*^{tm1CAM} mice, much less than the upstream probe. In wild-type mice, both probes detected approximately equivalent amounts of Cftr mRNA. Identical results were obtained from the 10-week-old *Cftr*^{tm1CAM} mice. These data suggest the presence of significant levels of the truncated Cftr mRNA (Fig. 1a) in the Brunner's glands of *Cftr*^{tm1CAM}/*Cftr*^{tm1CAM} mice, and a low level of read-through of the introduced transcription termination signals. *Cftr* expression in the intestinal crypt epithelia of 3- to 4-week-old and 10-week-old mice was similar to that observed in neonatal mice. Both upstream and downstream probes detected 4-fold reduced Cftr mRNA expression in the ileal crypts of 10-week-old *Cftr*^{tm1CAM}/*Cftr*^{tm1CAM} mice, as compared with age-matched +/+ mice.

The salivary glands are also a major site of *Cftr* expression (25,28). Similar levels of Cftr mRNA were detected with both the Cftr probes in the intra- and interlobular ducts of the salivary glands of neonatal, +/+ mice (data summarised in Table 1). In *Cftr*^{tm1CAM}/*Cftr*^{tm1CAM} mice, the upstream probe detected Cftr mRNA in the intra- and interlobular salivary gland ducts, while the downstream Cftr probe did not detect Cftr mRNA expression. This pattern of expression is similar to that seen in the intestinal Brunner's glands of the *Cftr*^{tm1CAM} mice, and again suggests the presence of the truncated Cftr mRNA (Fig. 1a) in the salivary gland ducts of *Cftr*^{tm1CAM}/*Cftr*^{tm1CAM} mice.

Mdr1 expression in *Cftr*^{tm1CAM} mice

Co-ordinate regulation of *Cftr* and *Mdr1* would predict that alterations in the expression of one gene would lead to subsequent changes in the expression of the other. In rodents, the homologue of the human *MDR1* gene has been duplicated and the two mouse genes are designated *Mdr1a* and *Mdr1b* (also known as *Mdr3* and *Mdr1*, respectively, ref. 11). Since we are interested in combined *Mdr1a* and *Mdr1b* expression in the *Cftr*^{tm1CAM} mice, we used a probe which hybridised to both *Mdr1a* and *Mdr1b* sequences. We will refer to mouse *Mdr1* expression throughout to denote combined *Mdr1a* and/or *Mdr1b* expression. The sequences of exon 6 of mouse *Mdr1a* and *Mdr1b* contain only five differences out of 192 bp, so exon 6 of mouse *Mdr1b* was used to examine *Mdr1* expression. Southern blotting analysis demonstrated that this probe recognised both *Mdr1a* and *Mdr1b*, but not *Mdr2* (data not shown).

Table 1. Cftr mRNA expression in the intestines and salivary glands of wild-type (+/+) and *Cftr*^{tm1CAM}/*Cftr*^{tm1CAM} mice

Tissue and age	Genotype	Upstream Cftr probe	Downstream Cftr probe
Intestinal Brunner's glands	+/+	++++	++++
(weaning and adult mice)	*Cftr*^{tm1CAM}/*Cftr*^{tm1CAM}	+++	+
Intestinal crypt epithelia	+/+	+++	+++
(weaning and adult mice)	*Cftr*^{tm1CAM}/*Cftr*^{tm1CAM}	+ (4-fold reduced)	+ (4-fold reduced)
Salivary gland ducts	+/+	+++	+++
(neonates)	*Cftr*^{tm1CAM}/*Cftr*^{tm1CAM}	+++	–

Relative signal intensities: ++++ = high; +++ = moderate; ++ = low; + = just detectable; – = not detectable.
Age groups: neonatal = 1–3 days; weaning = 3–4 weeks; adult = 10 weeks.

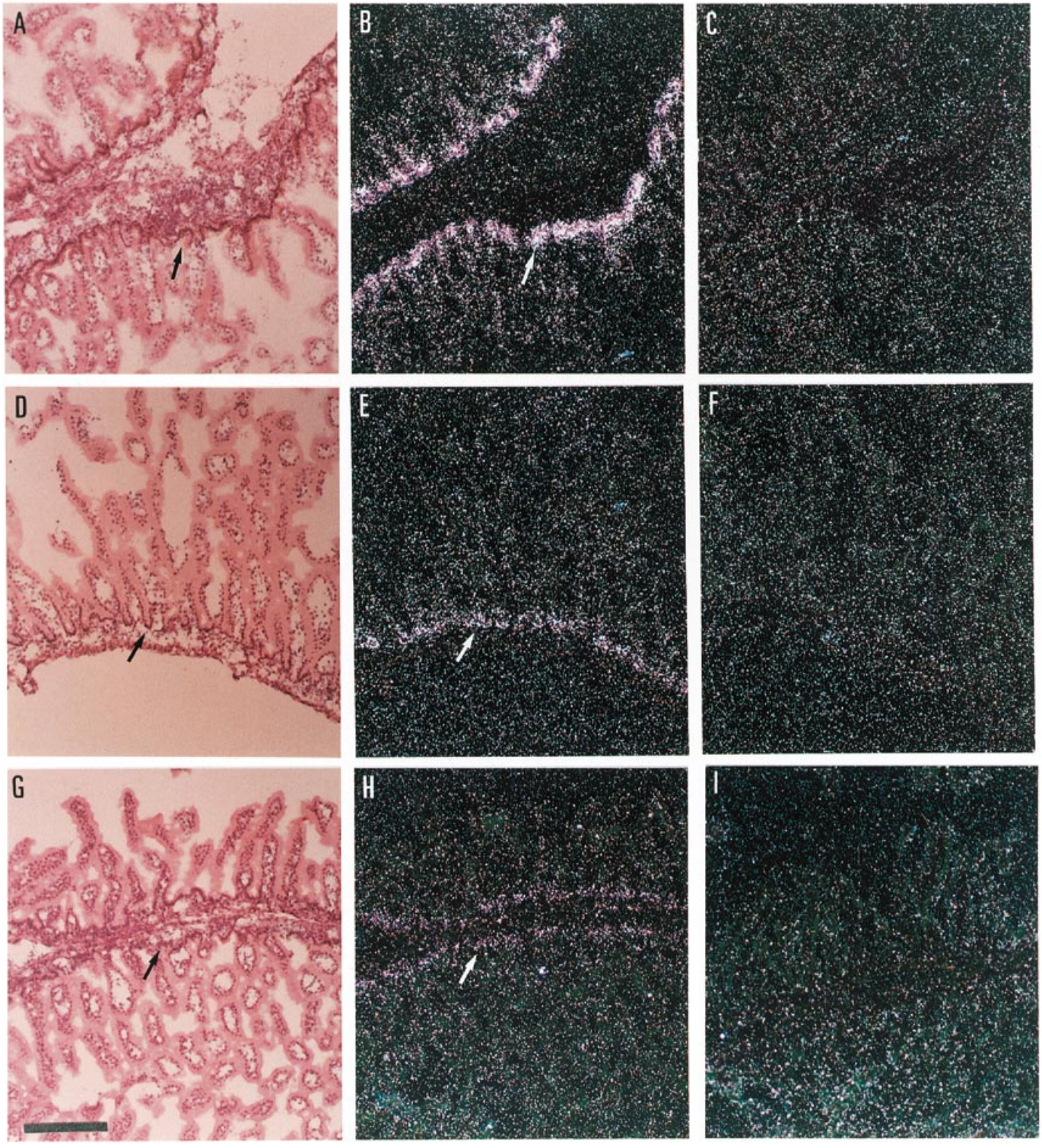

Figure 4. Cftr mRNA expression in 1-day-old, *Cftr*^{tm1CAM} mice. (**A**, **D** and **G**) Brightfield images of cryostat sections of the small intestine that have been hybridised to the antisense, upstream Cftr probe. Arrows indicate intestinal intervillous epithelia, from which the intestinal crypts will develop during post-natal weeks 1 and 2. (**B**, **E** and **H**) Darkfield images of the same sections allowing visualisation of the hybridisation signal (white dots). The intensity of the hybridisation signal gives an indication of the amount of mRNA present. (**C**, **F** and **I**) Darkfield images of consecutive sections hybridised with the corresponding sense strand probe, which serves as a negative control. The sections in (A), (B) and (C) are from a +/+ mouse, those in (D), (E) and (F) from a +/*Cftr*^{tm1CAM} mouse and those in (G), (H) and (I) from a *Cftr*^{tm1CAM}/*Cftr*^{tm1CAM} mouse. The size bar equals 200 µm.

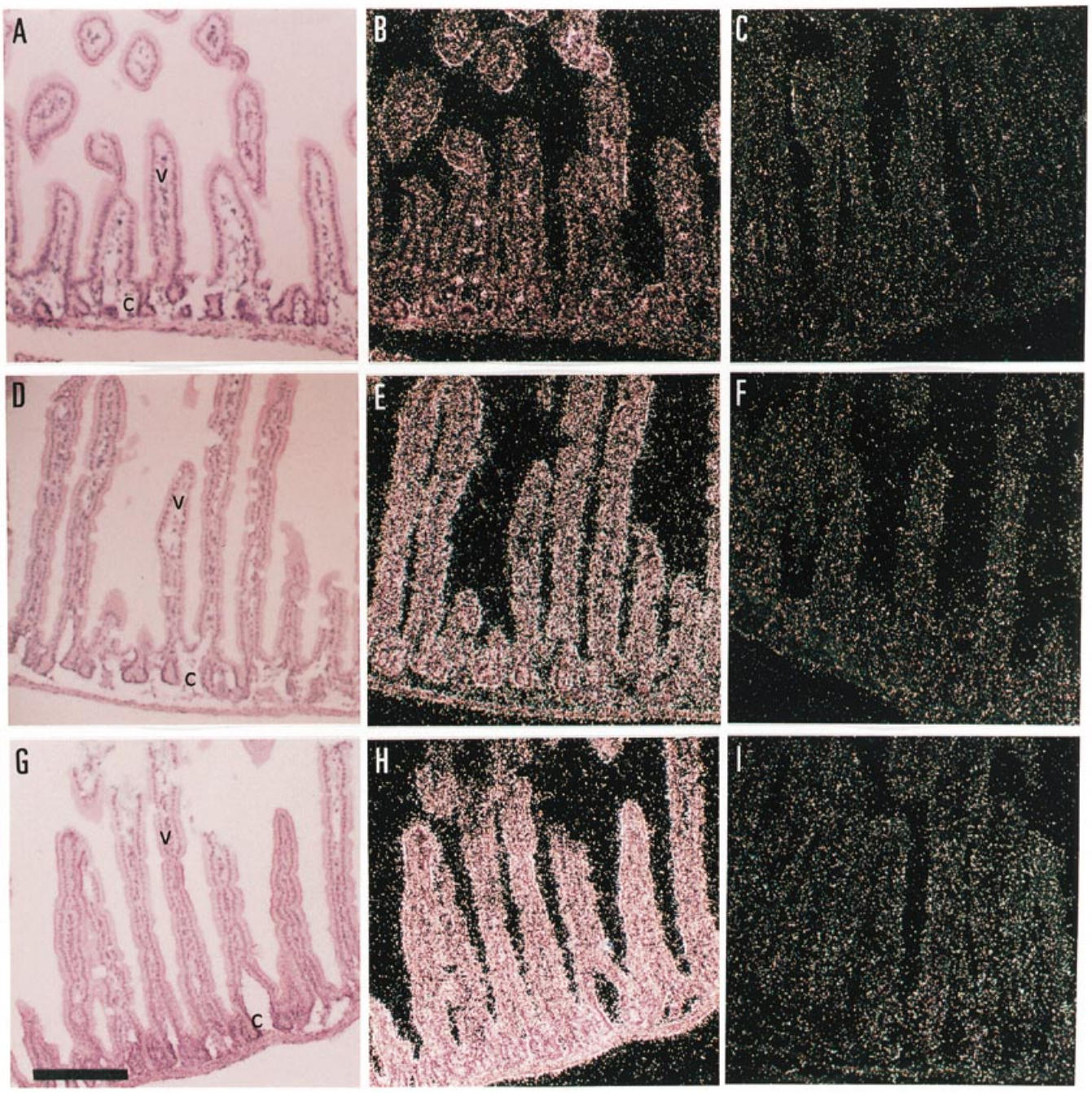

Figure 5. *Mdr1* expression in the intestinal crypt (c) and villous (v) epithelia of 3- to 4-week-old *Cftr*^{tm1CAM} mice. (**A**, **D** and **G**) Brightfield images of sections hybridised to an antisense Mdr1 probe; (**B**, **E** and **H**) show darkfield images of these sections. (**C**, **F** and I) Darkfield images of consecutive sections hybridised to the sense Mdr1 probe. *Mdr1* expression in +/+, +/*Cftr*^{tm1CAM} and *Cftr*^{tm1CAM}/*Cftr*^{tm1CAM} mice is shown in (A–C), (D–F) and (G–I), respectively. The size bar equals 200 µm.

Reduced levels of Cftr mRNA expression were observed in the intestines of 1-day-old and 3- to 4-week-old *Cftr*^{tm1CAM}/*Cftr*^{tm1CAM} mice (Fig. 4). Therefore, *Mdr1* expression was studied in a series of consecutive sections. The cellular patterns of *Cftr* and *Mdr1* expression observed in 3- to 4-week-old mice were similar to those found in the 1-day-old mice. In +/+ mice of both age groups, low levels of Mdr1 mRNA were observed in the intestinal intervillous and villous epithelia (Fig. 5A and B). The expression of *Mdr1* in both intervillous and villous epithelial cells differed from the pattern of expression in adult +/+ mice where expression was restricted to the villous epithelia (ref. 15, and see Fig. 6). In 1-day-old and 3- to 4-week-old *Cftr*^{tm1CAM}/*Cftr*^{tm1CAM} mice, Mdr1 mRNA expression was also observed in intervillous and villous epithelia, but the level of *Mdr1* expression was increased 4-fold compared with +/+ mice (Fig. 5G and H). We also examined intestinal *Mdr1* expression in 3- to 4-week-old heterozygous mice. The cellular distribution of Mdr1 mRNA was identical in all three mouse genotypes, and an intermediate level

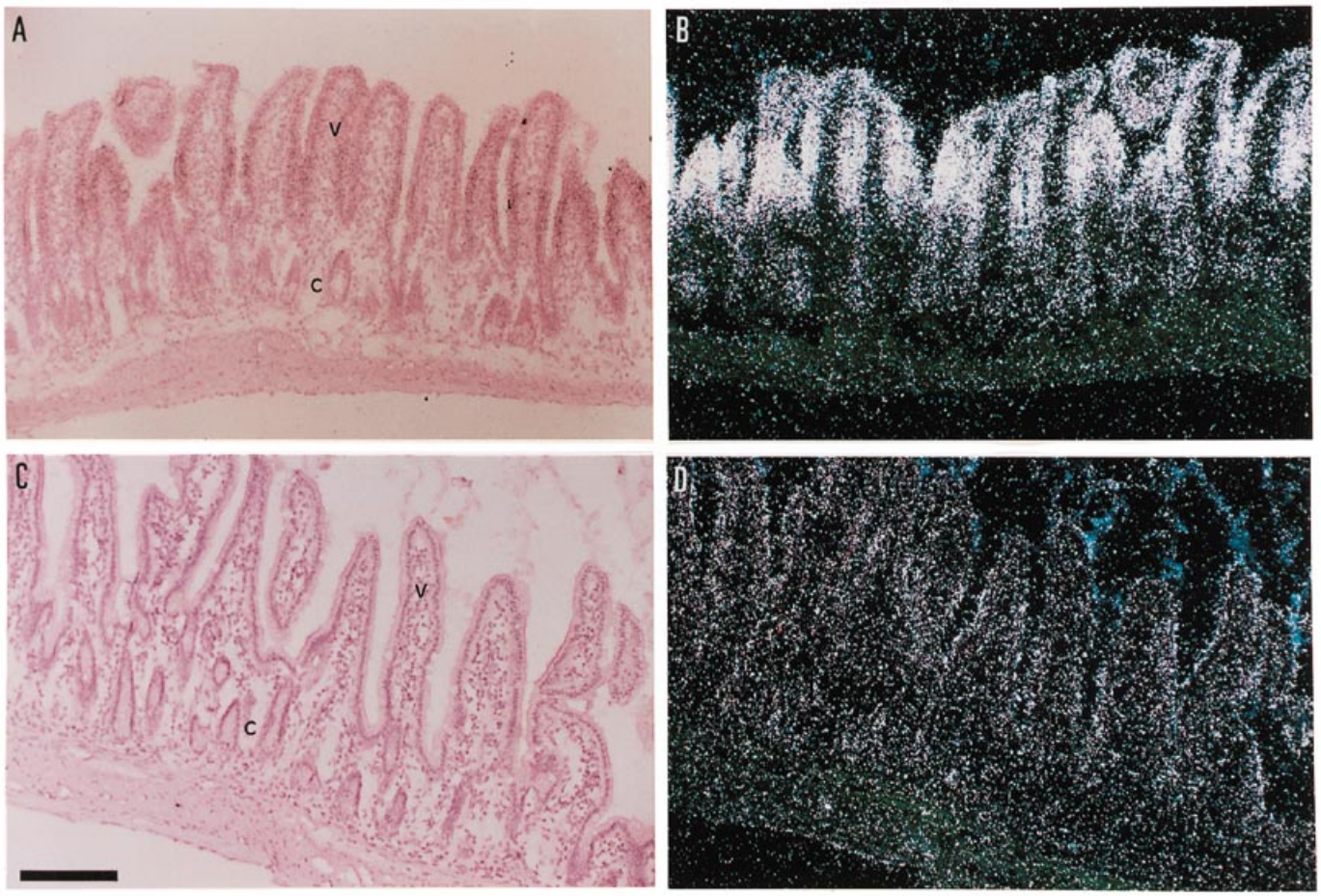

Figure 6. *Mdr1* expression in the ileum of 10-week-old $Cftr^{tm1CAM}$ mice. (**A** and **B**) *Mdr1* expression in the villous (V), but not the crypt epithelia (C) of a +/+ mouse. (**C** and **D**) *Mdr1* expression is greatly reduced in the ileum of a $Cftr^{tm1CAM}/Cftr^{tm1CAM}$ mouse. (A) and (C) show brightfield images of sections hybridised to the antisense Mdr1 probe while (B) and (D) show the corresponding darkfield images. The size bar equals 100 µm.

of *Mdr1* expression was observed in the $+/Cftr^{tm1CAM}$ mice as compared with +/+ and $Cftr^{tm1CAM}/Cftr^{tm1CAM}$ mice (Fig. 5, compare E with B and H, respectively).

To determine whether the changes in *Mdr1* expression observed in 1-day-old and 3- to 4-week-old $Cftr^{tm1CAM}/Cft^{tm1CAM}$ mice were affected by intestinal development, we also examined *Mdr1* expression in 10-week-old (adult) $Cftr^{tm1CAM}$ mice. In adult +/+ mice, *Mdr1* expression was restricted to the duodenal and ileal villous epithelia with no evidence of expression in the crypt epithelia or Brunner's glands (Fig. 6A and B and data not shown), typical of the mature pattern of intestinal *Mdr1* expression (15). Comparison of Mdr1 mRNA expression in all three age groups of +/+ mice revealed a gradual contraction in expression from the intervillous/crypt and villous epithelia seen in mice up to the age of weaning, to the villous epithelia of adult mice. There was also an increase in the level of *Mdr1* expression in the villous epithelia after weaning was complete. In contrast to our observations in the younger $Cftr^{tm1CAM}/Cftr^{tm1CAM}$ mice, we observed a marked decrease in Mdr1 mRNA expression in the duodenal and ileal villous epithelia of 10-week-old $Cftr^{tm1CAM}/Cftr^{tm1CAM}$ mice (Fig. 6C and D), as compared with +/+ mice (Fig. 6A and B). The levels of Mdr1 mRNA were 3-fold less in the small intestines of 10-week-old $Cftr^{tm1CAM}/Cftr^{tm1CAM}$ mice, compared with +/+ mice. Our observations suggest that the transition through weaning results in Mdr1 mRNA expression changing from overexpression in immature $Cftr^{tm1CAM}/Cftr^{tm1CAM}$ intestine, to underexpression in adult $Cftr^{tm1CAM}/Cftr^{tm1CAM}$ intestine. This is in contrast to the developmental changes in *Mdr1* expression in +/+ intestine, where an overall increase in Mdr1 mRNA levels was observed after weaning.

To establish that the changes in *Mdr1* expression observed in the $Cftr^{tm1CAM}/Cftr^{tm1CAM}$ mice are specific to the loss of *Cftr* expression and/or function, and not a result of a general alteration in expression of all genes in the $Cftr^{tm1CAM}/Cftr^{tm1CAM}$ mice, we examined *Mdr2* and *Pgk-1* expression in 3- to 4-week-old and 10-week-old $Cftr^{tm1CAM}$ mice (Fig. 7). The mouse Mdr2 probe recognised *Mdr2* exon 21, and Southern blotting showed that this probe hybridised specifically to mouse *Mdr2*, but not to *Mdr1a* or *Mdr1b* (data not shown). A human PGK-1 probe, which cross-hybridises with mouse Pgk-1 sequences (29), was used to assess mouse *Pgk-1* expression.

Mdr2 is not normally expressed in the intestine (30) and no transcripts were detected in the intestines of either +/+ or $Cftr^{tm1CAM}/Cftr^{tm1CAM}$ mice (data not shown). *Pgk-1* was found to be expressed in the duodenal and ileal crypt and villous epithelia (Fig. 7). The highest level of Pgk-1 mRNA was observed in the crypt epithelia, with a decreasing gradient of

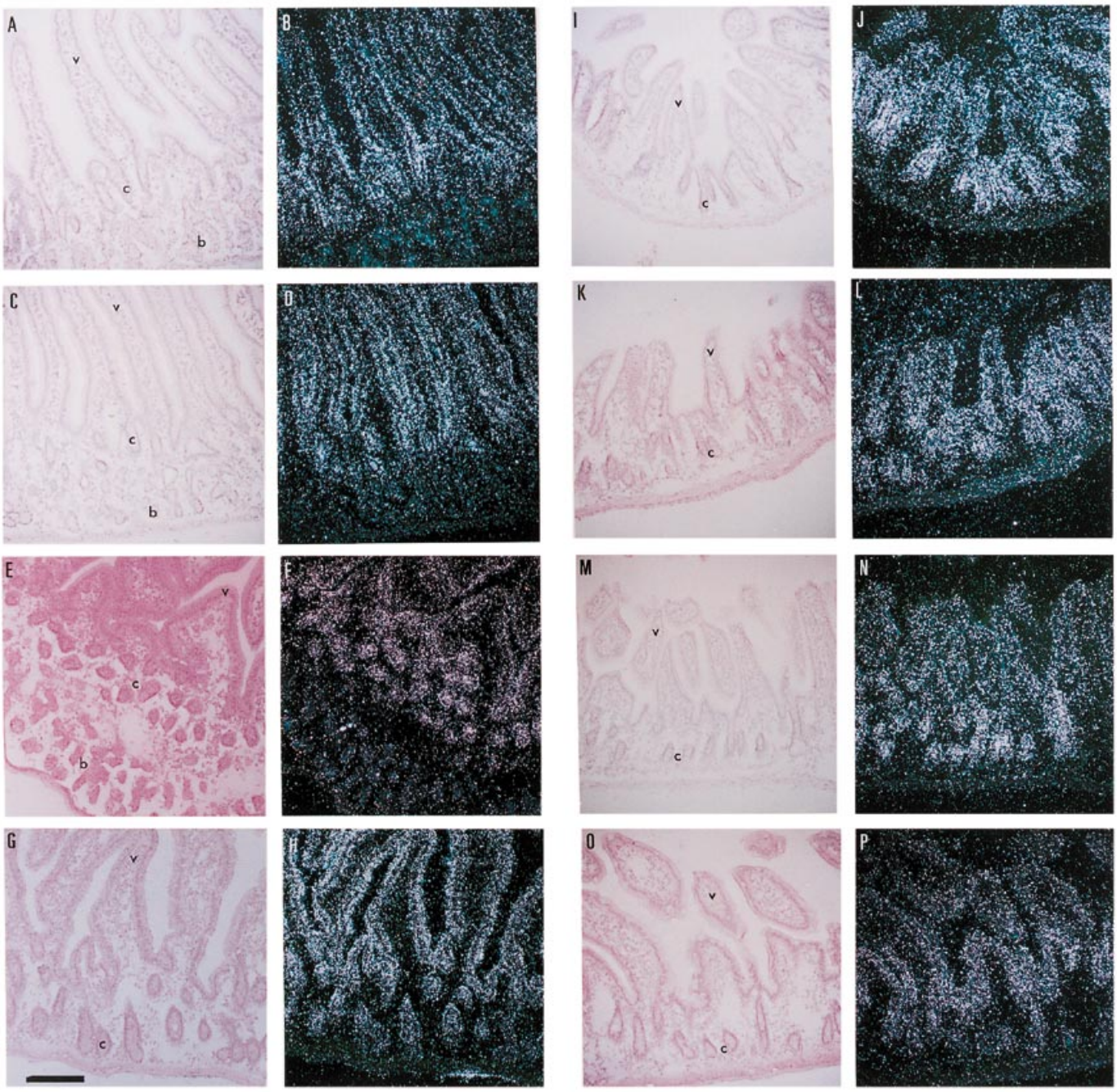

Figure 7. *Pgk-1* expression in the duodenum (A–H) and ileum (I–P) of 3- to 4-week-old, and 10-week-old *Cftr*^{tm1CAM} mice. The intestinal crypts (c), villi (v) and Brunner's glands (b) are marked. (**A**, **C**, **E**, **G**, **I**, **K**, **M** and **O**) Brightfield images of sections hybridised to the PGK-1 probe. (**B**, **D**, **F**, **H**, **J**, **L**, **N** and **P**) Darkfield images of these same sections. Sections in (A), (B), (E), (F), (I), (J), (M) and (N) are from a +/+ mouse and sections in (C), (D), (G), (H), (K), (L), (O) and (P) are from a *Cftr*^{tm1CAM}/*Cftr*^{tm1CAM} mouse. The sections in (A–D) and (I–L) are from 3- to 4-week-old mice and the sections in (E–H) and (M–P) are from 10-week old-mice. The size bar equals 200 μm.

expression along the crypt–villous axis. Pgk-1 mRNA was not detected in the Brunner's glands of the intestine (Fig. 7A–H). In both age groups of *Cftr*^{tm1CAM} mice, the level and cellular distribution of expression of Pgk-1 mRNA in the intestine was similar in +/+ and *Cftr*^{tm1CAM}/*Cftr*^{tm1CAM} mice (Fig. 7). Therefore, we conclude that the changes in *Mdr1* expression observed in the *Cftr*^{tm1CAM}/*Cftr*^{tm1CAM} mice are specific to the loss of *Cftr* expression and/or function.

DISCUSSION

Cftr expression in *Cftr*^{tm1CAM} mice

The *Cftr*^{tm1CAM} mice were produced by a replacement targeting event in which an *HPRT*^{R} mini-gene was inserted into exon 10 of the *Cftr* locus. RT-PCR, RNase protection and RNA *in situ* hybridisation data suggest the level of read-through of the *HPRT*^{R}

mini-gene is low and that the majority of the Cftr mRNA detected in the *Cftr*^{tm1CAM}/*Cftr*^{tm1CAM} mice is the truncated Cftr mRNA shown in Figure 1a. We were able to detect the truncated Cftr mRNA (Fig. 1a) in the Brunner's glands and salivary gland ducts, but not in the intestinal crypt epithelia of the *Cftr*^{tm1CAM}/*Cftr*^{tm1CAM} mice. *Cftr* is expressed at similar levels in the salivary gland ducts and intestinal crypt epithelia of wild-type mice. This suggests tissue-specific differences in the stability of the truncated Cftr mRNA, and that the truncated mRNA is less stable than wild-type Cftr mRNA in crypt epithelia. This is not surprising since exons 11–24 and the 3′ untranslated region (3′ UTR) have been deleted, and the 3′ UTR often contains sequence motifs important in determining mRNA stability (31). This finding suggests that the 3′ UTR may also be important for Cftr mRNA stability in some cell types. It is also possible that the alterations in Cftr mRNA levels may be due to changes in the rate of transcription initiation from the *Cftr*^{tm1CAM} promoter, and that these changes in transcription are further complicated by the altered stability of the mutant Cftr mRNAs. As the disruption of the *Cftr*^{tm1CAM} locus is contained entirely within exon 10 it is unlikely that this event alters the rate of transcription initiation from the *Cftr*^{tm1CAM} promoter, although this has not been demonstrated formally. Overall, these studies show that Cftr mRNA levels are greatly reduced in the *Cftr*^{tm1CAM}/*Cftr*^{tm1CAM} mice and any Cftr mRNA expressed is largely terminated at the targeted interruption.

Mdr1 expression in the *Cftr*^{tm1CAM} mice

The data presented here show that *Mdr1* expression is developmentally regulated in the intestines of wild-type mice. In neonatal and suckling–weaning mice, *Mdr1* was expressed at low levels throughout the intervillous/crypt and villous epithelia, while in adult mice the level of *Mdr1* expression was increased and restricted to the villous epithelia. The transition through weaning is a crucial stage of intestinal development and is known to produce changes in the expression of a number of genes that play important roles in intestinal physiology (32,33). The developmental regulation of *Mdr1* expression in the intestine is consistent with such a role for Mdr1 in normal intestinal function.

We have shown previously that *Cftr* and *Mdr1* exhibit complementary patterns of expression *in vivo*, suggesting that the regulation of expression of the two genes may be co-ordinated (15). The results of this study provide further evidence for the co-ordinate regulation of *Cftr* and *Mdr1* expression *in vivo*.

In the intestinal epithelia of neonatal (1-day-old) and suckling–weaning (3- to 4-week-old) *Cftr*^{tm1CAM}/*Cftr*^{tm1CAM} mice, Mdr1 mRNA expression was increased compared with wild-type mice, while in adult *Cftr*^{tm1CAM}/*Cftr*^{tm1CAM} mice *Mdr1* was underexpressed. The expression of two control genes was not altered in the *Cftr*^{tm1CAM}/*Cftr*^{tm1CAM} mice, indicating that the observed changes in *Mdr1* expression were specific to the loss of *Cftr* expression/function. We also observed intermediate levels of *Mdr1* expression in +/*Cftr*^{tm1CAM} mice, suggesting that alterations in Mdr1 mRNA levels are regulated in response to decreased *Cftr* expression and/or function. Furthermore, as the +/*Cftr*^{tm1CAM} mice are phenotypically wild-type (19), this suggests that the changes in *Mdr1* expression are not due to a general stress response associated with the severe intestinal phenotype of the *Cftr*^{tm1CAM}/*Cftr*^{tm1CAM} mice. The changes in *Mdr1* expression observed in the *Cftr*^{tm1CAM}/*Cftr*^{tm1CAM} mice are also influenced by the developmental stage of the intestine. The transition through weaning results in *Mdr1* expression in *Cftr*^{tm1CAM}/*Cftr*^{tm1CAM} intestines changing from overexpression to underexpression, suggesting that the co-ordinate regulation of *Cftr* and *Mdr1* expression is also subject to temporal regulation associated with weaning.

As only a small percentage of *Cftr*^{tm1CAM}/*Cftr*^{tm1CAM} mice survive to 10 weeks, it is possible that these mice may represent a sub-population, and that down-regulation of *Mdr1* expression in 10-week-old *Cftr*^{tm1CAM}/*Cftr*^{tm1CAM} mice does not represent the true pattern of *Mdr1* expression in the general population of adult *Cftr*^{tm1CAM} mice. If this were the case then we would expect to see some immature *Cftr*^{tm1CAM}/*Cftr*^{tm1CAM} mice showing underexpression of *Mdr1* in their intestines. We analysed *Mdr1* expression in nine neonatal and suckling–weaning *Cftr*^{tm1CAM}/*Cftr*^{tm1CAM} mice and always observed increased intestinal *Mdr1* expression. For similar reasons, we suggest that the modifier locus, which modulates the severity of the cystic fibrosis phenotype in the *Cftr*^{tm1HSC} mice (22), is unlikely to have an impact on *Mdr1* expression in the *Cftr*^{tm1CAM} mice.

This work, together with our previous studies of the expression of *Cftr* and *Mdr1*, suggests that the expression of both these genes is subject to spatial, hormonal, temporal and co-ordinate regulation (15,26,34). A number of possible mechanisms underlying the co-ordinated regulation of *Cftr* and *Mdr1* can be envisaged. It is possible that a reduction or loss of Cftr function influences Mdr1 mRNA expression. This model is consistent with the observation of increased *Mdr1* expression in the *Cftr*^{tm1CAM}/*Cftr*^{tm1CAM} mice, which express no functional Cftr protein, and the intermediate increase in Mdr1 mRNA levels in +/*Cftr*^{tm1CAM} mice. However, it is equally possible that some other aspect of *Cftr* expression influences *Mdr1* expression, for example mRNA levels. Any proposed model will also have to take into account the interaction between mechanisms directing the co-ordinate regulation of *Cftr* and *Mdr1* and the temporal regulation of *Mdr1*.

MATERIALS AND METHODS

Mice and reagents

The population of cystic fibrosis knockout mice was created and bred at the Wellcome/CRC Institute in Cambridge (*Cftr*^{tm1CAM} mice). The genotypes of the mice were established by PCR and Southern blot analysis as described previously (18,19)

In situ hybridisation

Animals were sacrificed by a lethal injection of anaesthetic and tissues fixed by whole body perfusion with 4% paraformaldehyde. *In situ* hybridisation was carried out essentially as described previously (26). Cryostat sections (10 μm) were hybridised to ^{35}S-labelled, single-stranded RNA probes. The antisense strand probe will hybridise to the mRNA and identify cells expressing the gene of interest. The sense strand probe serves as a negative control.

The upstream and downstream mouse Cftr probes were generated by PCR and have been described previously (26). The mouse Mdr1b exon 6 probe was produced by PCR amplification from the mouse Mdr1b cDNA (a generous gift from Dr P. Gros). The sequence of the PCR DNA fragment exactly matched the published mouse *Mdr1b* sequence, and corresponded to nucleotides 446–635 (35). The mouse Mdr2 exon 21 probe was

generated by PCR from mouse genomic DNA. The sequence of the mouse Mdr2 exon 21 probe exactly matched the published mouse *Mdr2* sequence and corresponded to positions 2663–2864 (36). The human PGK-1 probe, which cross-hybridises with mouse Pgk-1 sequences, corresponded to 68 bp of intron 2 and 121 bp of exon 3 of human *PGK-1*. The plasmid containing the human PGK-1 insert was kindly provided by Dr J. Firth (29). All DNA fragments used as *in situ* hybridisation probes were subcloned into pSK+ (Bluescript: Stratagene) to allow the *in vitro* transcription of the insert using T3 and T7 RNA polymerases.

In situ hybridisation signal intensities were estimated by densitometric analysis of contact sheets of *in situ* hybridisation slides made prior to dipping the slides in photographic emulsion. Contact sheets were obtained using Amersham β-max film and hybridisation signal intensities quantitated using an Seescan densitometer (Cambridge, UK). Hybridisation signals from a given probe were quantitated by averaging readings from a minimum of three sections per probe per animal. In the case of +/+, 1-day-old animals, measurements from two animals were averaged to a give a final measure of the level of signal from a given probe. In all other cases, measurements were averaged from three animals.

Total RNA preparation, reverse transcription-PCR and RNase protection analysis

Total RNA was prepared using either the acid guanidinium thiocyanate phenol method (37), or by lithium chloride urea extraction (38).

RT-PCR was carried out according to (39). Two pairs of primers were used. One pair amplified a fragment of 480 bp, containing exons 4–6 of murine *Cftr* upstream of the targeted interruption in exon 10 of the *Cftr*^{tm1CAM} mice. The other pair of primers amplified a fragment of 375 bp, corresponding to exons 11–13 downstream of the targeted disruption. A pair of primers which amplified a 500 bp fragment of β-actin cDNA (40) were used as a positive control.

The primers for *Cftr* exons 4–6 were: SM3, 5′-tccag cctgt cttgc tagga agaat-3′ and SM4, 5′-cattg atctt tgcag ctctt tgatc-3′. The primers for *Cftr* exons 11–13 were: X11F, 5′-GACAT CACCA AGTTT GCAGA A-3′ and SDCF4, 5′-AAACT GGTCA AAAGT ATCAT AC-3′. The primers for β-actin were: Actin 1, 5′-ATGGA TGACG ATATC GCTG-3′ and Actin 2, 5′-ACCTG ACAGA CTACC TCAT-3′.

RNase protection assays were performed using standard techniques (41) except that tRNA was omitted from the reaction. After digestion with RNase A and T1, the digestion products were electrophoresed on denaturing, 10% polyacrylamide gels and protected fragments were visualised by autoradiography. The plasmid pE16 was generated by ligation of a 791 bp *Sau*3AI–*Nsi*I fragment, containing the whole of the mouse *Cftr* exon 10 as well as some flanking intron sequence, into the *Bam*HI–*Pst*I sites of pT7/T3α-19 (Gibco BRL). Plasmid p987 was generated by ligation of a 906 bp *Bgl*II–*Nsi*I fragment derived from pCFB-HPRT (18) into the *Bam*HI–*Pst*I sites of pT7/T3α-19. p987 therefore contains only that part of mouse exon 10 which is downstream of the *HPRT* insertion plus some flanking intron 10 sequence. Riboprobes were generated from these plasmids for RNase protection assays using T7 RNA polymerase according to the manufacturer's instructions.

ACKNOWLEDGEMENTS

We thank Drs Kevin Spring, Lis Mudd, Simon Hardy, Jay Hinton and Miss Nina Birchall for advice and discussions. A.E.O.T. was a Beit Memorial Research Fellow during the course of this research and C.F.H. is a Howard Hughes International Research Scholar. This research was supported by the Wellcome Trust, the Henry Smith Foundation, the Cystic Fibrosis Research Trust, the Imperial Cancer Research Fund and the Medical Research Council.

REFERENCES

1. Rommens, J.M., Iannuzzi, M.C., Kerem, B.-S., Drumm, M.L., Melmer, G., Dean, M., Rozmahel, R., Cole, J.L., Kennedy, D., Hidaka, N., Zsiga, M., Buchwald, M., Riordan, J.R., Tsui, L.-C. and Collins, F.S. (1989) Identification of the cystic fibrosis gene: chromosome walking and jumping. *Science*, **245**, 1059–1065.
2. Riordan, J.R., Rommens, J.M., Kerem, B.-S., Alon, N., Rozmahel, R., Grzelczak, Z., Zielenski, J., Lok, S., Plavsic, N., Chou, J.-L., Drumm, M.L., Iannuzzi, M.C., Collins, F.S. and Tsui, L.-C. (1989) Identification of the cystic fibrosis gene: cloning and characterization of complementary DNA. *Science*, **245**, 1066–1073.
3. Kerem, B.-S., Rommens, J.M., Buchanan, J.A., Markiewicz, D., Cox, T.K., Chakravarti, A., Buchwald, M. and Tsui, L.-C. (1989) Identification of the cystic fibrosis gene: genetic analysis. *Science*, **245**, 1073–1080.
4. Boat, T.F., Welsh, M.J. and Beaudet, A.L. (1989) Cystic fibrosis. In Scriver, C.R., Beaudet, A.L., Sly, W.S and Valle, D. (eds), *The Metabolic Basis of Inherited Disease*. McGraw-Hill, New York. pp. 2649–2680.
5. Anderson, M.P., Gregory, R.J., Thompson, S., Souza, D.W., Paul, S., Mulligan, R.C., Smith, A.E. and Welsh, M.J. (1991) Demonstration that CFTR is a chloride channel by alteration of its anion selectivity. *Science*, **253**, 202–205.
6. Gray, M.A., Harris, A., Coleman, L., Greenwell, J.R. and Argent, B.E. (1989) Two types of chloride channel on duct cells cultured from human foetal pancreas. *Am. J. Physiol.*, **257**, C240–C251.
7. Bear, C.E., Li, C.H., Kartner, N., Bridges, R.J., Jensen, T.J., Ramjeesingh, M. and Riordan, J.R. (1992) Purification and functional reconstitution of the cystic fibrosis transmembrane conductance regulator (CFTR). *Cell*, **68**, 809–818.
8. Egan, M., Flotte, T., Afione, S., Solow, R., Zeitlin, P.L., Carter, B.J. and Guggino, W.B. (1992) Defective regulation of outwardly rectifying Cl^- channels by protein kinase A corrected by insertion of CFTR. *Nature*, **358**, 581–584.
9. Stutts, M.J., Canessa, C.M., Olsen, J.C., Hamrick, M., Cohn, J.A., Rossier, B.C. and Boucher, R.C. (1995) CFTR as a cAMP-dependent regulator of sodium channels. *Science*, **269**, 847–850.
10. Higgins, C.F. (1992) ABC transporters: from microorganisms to man. *Annu. Rev. Cell Biol.*, **8**, 67–113.
11. Gottesman, M.M. and Pastan, I. (1993) Biochemistry of multidrug resistance mediated by the multidrug transporter. *Annu. Rev. Biochem.*, **62**, 385–427.
12. Valverde, M.A., Diaz, M., Sepulveda, F.V., Gill, D.R., Hyde, S.C. and Higgins, C.F. (1992) Volume-regulated chloride channels associated with the human multidrug-resistance P-glycoprotein. *Nature*, **355**, 830–833.
13. Hardy, S.P., Goodfellow, H.R., Valverde, M.A., Gill, D.R., Sepulveda, V. and Higgins, C.F. (1995) Protein kinase C-mediated phosphorylation of the human multidrug resistance P-glycoprotein regulates cell volume-activated chloride channels. *EMBO J.*, **14**, 68–75.
14. Valverde, M.A., Bond, T.D., Hardy, S.P., Taylor, J.C., Higgins, C.F., Altamirano, J. and Alverez-Leefmans, F.J. (1996) The multidrug resistance P-glycoprotein modulates cell regulatory volume decrease. *EMBO J.*, **15**, 4460–4469.
15. Trezise, A.E., Romano, P.R., Gill, D.R., Hyde, S.C., Sepulveda, F.V., Buchwald, M. and Higgins, C.F. (1992) The multidrug resistance and cystic fibrosis genes have complementary patterns of epithelial expression. *EMBO J.*, **11**, 4291–4303.
16. Bremer, S., Hoof, T., Wilke, M., Busche, R., Scholte, B., Riordan, J.R., Maass, G. and Tummler, B. (1992) Quantitative expression patterns of multidrug-resistance P-glycoprotein (MDR1) and differentially spliced cystic-fibrosis transmembrane-conductance regulator mRNA transcripts in human epithelia. *Eur. J. Biochem.*, **206**, 137–149.

17. Breuer, W., Slotki, I.N., Ausiello, D.A. and Cabantchik, I.Z. (1993) Induction of multidrug-resistance down-regulates the expression of cftr in colon epithelial-cells. *Am. J. Physiol.*, **265**, C1711–C1715.
18. Colledge, W.H., Ratcliff, R., Foster, D., Williamson, R.and Evans, M.J. (1992) Cystic fibrosis mouse with intestinal obstruction. *Lancet*, **340**.
19. Ratcliff, R., Evans, M.J., Cuthbert, A.W., MacVinish, L.J., Foster, D., Anderson, J.R. and Colledge, W.H. (1993) Production of a severe cystic fibrosis mutation in mice by gene targeting. *Nature Genet.*, **4**, 35–41.
20. Snouwaert, J.N., Brigman, K.K., Latour, A.M., Malouf, N.N., Boucher, R.C., Smithies, O. and Koller, B.H. (1992) An animal model for cystic fibrosis made by gene targeting. *Science*, **257**, 1083–1088.
21. O'Neal, W.K., Hasty, P., McCray, P.J., Casey, B., Rivera, P.J., Welsh, M.J., Beaudet, A.L. and Bradley, A. (1993) A severe phenotype in mice with a duplication of exon 3 in the cystic fibrosis locus. *Hum. Mol. Genet.*, **2**, 1561–1569.
22. Rozmahel, R., Wilschanski, M., Matin, A., Plyte, S., Oliver, M., Auerbach, W., Moore, A., Forstner, J., Durie, P., Nadeau, J., Bear, C. and Tsui, L.-C. (1996) Modulation of disease severity in cystic fibrosis transmembrane conductance regulator deficient mice by a secondary genetic factor. *Nature Genet.*, **12**, 280–287.
23. Dorin, J.R., Dickinson, P., Alton, E.W., Smith, S.N., Geddes, D.M., Stevenson, B.J., Kimber, W.L., Fleming, S., Clarke, A.R., Hooper, M.L., Anderson, L., Beddington, R.S.P. andPorteous, D.J. (1992) Cystic fibrosis in the mouse by targeted insertional mutagenesis. *Nature*, **359**, 211–215.
24. Winpenny, J.P., Verdon, B., McAlroy, H.L., Colledge, W.H., Ratcliff, R., Evans, M.J., Gray, M.A. and Argent, B.E. (1995) Calcium-activated chloride conductance is not increased in pancreatic duct cells of CF mice. *Pflugers Arch.*, **430**, 26–33.
25. Trezise, A.E. and Buchwald, M. (1991) *In vivo* cell-specific expression of the cystic fibrosis transmembrane conductance regulator. *Nature*, **353**, 434–437.
26. Trezise, A.E., Linder, C.C., Grieger, D., Thompson, E.W., Meunier, H., Griswold, M.D. and Buchwald, M. (1993) CFTR expression is regulated during both the cycle of the seminiferous epithelium and the oestrous cycle of rodents. *Nature Genet.*, **3**, 157–164.
27. Tata, F., Stanier, P., Wicking, C., Halford, S., Kruyer, H., Lench, N.J., Scambler, P.J., Hansen, C., Braman, J.C., Williamson, R. and Wainwright, B.J. (1991). Cloning the mouse homolog of the human cystic fibrosis transmembrane conductance regulator gene. *Genomics*, **10**, 301–307.
28. Kartner, N., Augustinas, O., Jensen, T.J., Naismith, A.L. and Riordan, J.R. (1992) Mislocalization of delta F508 CFTR in cystic fibrosis sweat gland. *Nature Genet.*, **1**, 321–327.
29. Firth, J.D., Ebert, B.L., Pugh, C.W. and Ratcliffe, P.J. (1994) Oxygen-regulated control elements in the phosphoglycerate kinase 1 and lactate dehydrogenase A genes: similarities with the erythropoietin 3′ enhancer. *Proc. Natl Acad. Sci. USA*, **91**, 6496–500.
30. Croop, J.M., Raymond, M., Haber, D., Devault, A., Arceci, R.J., Gros, P. and Housman, D.E. (1989) The three mouse multidrug resistance (mdr) genes are expressed in a tissue-specific manner in normal mouse tissues. *Mol. Cell. Biol.*, **9**, 1346–1350.
31. Jackson, R.J. (1993) Cytoplasmic regulation of mRNA function: the importance of the 3′ untranslated region. *Cell*, **74**, 9–14.
32. Birkenmeier, E.H. and Gordon, J.I. (1986) Developmental regulation of a gene that encodes a cysteine-rich intestinal protein and maps near the murine immunoglobulin heavy chain locus. *Proc. Natl Acad. Sci. USA*, **83**, 2516–2520.
33. Duluc, I., Jost, B. and Freund, J.-N. (1993) Multiple levels of the stage- and region-specific expression of rat intestinal lactase. *J. Cell Biol.*, **123**, 1577–1586.
34. Trezise, A.E., Chambers, J.A., Wardle, C.J., Gould, S. and Harris, A. (1993) Expression of the cystic fibrosis gene in human foetal tissues. *Hum. Mol. Genet.*, **2**, 213–218.
35. Gros, P., Croop, J. and Housman, D. (1986) Mammalian multidrug resistance gene: complete cDNA sequence indicates strong homology to bacterial transport proteins. *Cell*, **47**, 371–380.
36. Gros, P., Raymond, M., Bell, J.and Housman, D. (1988) Cloning and characterization of a second member of the mouse mdr gene family. *Mol. Cell. Biol.*, **8**, 2770–2778.
37. Chomczynski, P. and Sacchi, N. (1987) Single-step method of RNA isolation by acid guanidinium thiocyanate–phenol–chloroform extraction. *Anal. Biochem.*, **162**, 156–159.
38. Auffray, C. and Rougeon, F. (1980) Purification of mouse immunoglobulin heavy-chain messenger RNAs from total myeloma tumor RNA. *Eur. J. Biochem.*, **107**, 303–314.
39. Kawasaki, E.S. (1990) Amplification of RNA. In *PCR Protocols: A Guide to Methods and Applications.* Innis, M.A.,Gelfand, D.H., Shinsky, J.J. and White, T.J. (eds), Academic Press, pp. 21–27.
40. Tokunaga, K., Taniguchi, H., Yoda, K., Shimizu, M.and Sakiyama, S. (1986) Nucleotide sequence of a full-length cDNA for mouse cytoskeletal beta-actin mRNA. *Nucleic Acids Res.*, **14**.
41. Sambrook, J., Fritsch, E.F. and Maniatis, T. (1989) *Molecular Cloning: A Laboratory Manual.* Cold Spring Harbor Laboratory Press, Cold Spring Harbor, NY.